Conclusions

It has been demonstrated that DAB ligands are capable of using the maximum number of eight electrons for the coordination of the N=C—C=N skeleton toward binuclear metal carbonyl units. The first example of the η^2-C=N,η^2C=N′ coordination of the 1,4-diazabutadienes as a stable electronic structure in $Ru_2(CO)_4(DAB)(HC{\equiv}CH)$ should be taken into account when inter- or intramolecular exchange processes of the ligand are studied.[15]

We have shown recently that σ^2-N,η^2-N′,η^2-C=N′ coordination of the DAB ligand in $Ru_2(CO)_6(DAB)$ complexes lead to a remarkable activation of the η^2-C=N bond. Reaction of these complexes with free DAB ligands yielded $Ru_2(CO)_5(IAE)$ complexes (IAE = bis[(alkylimino)(alkylamino)ethane]) in which the IAE ligand consists of two DAB ligands linked together via a C–C bond between two imine carbon atoms.[12,13] It might be expected that η^2 coordination of both C=N bonds leads to the activation of both imine carbon centers in the ligand, giving new opportunities to the metal carbonyl supported synthesis of 1,2-disubstituted 1,2-diaminoethanes and related derivatives.

Acknowledgment. We wish to thank Mr. R. H. Fokkens for recording the mass spectra and Mr. D. Heijdenrijk for collecting the crystal data.

Registry No. $Ru_2(CO)_4$[glyoxal bis(isopropylimine)](HC≡CH), 75963-10-9; $Ru_2(CO)_4$[glyoxal bis(cyclohexylimine)](HC≡CH), 76822-76-9; $Ru_3(CO)_{12}$, 15243-33-1; $Ru_2(CO)_6$[glyoxal bis(isopropylimine)], 74552-69-5; $Ru_2(CO)_6$[glyoxal bis(cyclohexylimine)], 74552-70-8.

Supplementary Material Available: A list of temperature parameters and calculated structure factors (13 pages). Ordering information is given on any current masthead page.

Contribution from the Departments of Chemistry, The Johns Hopkins University, Baltimore, Maryland 21218, and Emory University, Atlanta, Georgia 30322

Coordination Chemistry of 7,9-Disubstituted 6-Oxopurine Metal Compounds. 3. Platinum(II) Coordination at N(1). Molecular and Crystal Structure of (Diethylenetriamine)(7,9-dimethylguanine)platinum(II) Hexafluorophosphate and (Diethylenetriamine)(7,9-dimethylhypoxanthine)platinum(II) Hexafluorophosphate Sesquihydrate[1]

BALTAZAR DE CASTRO, CHIAN C. CHIANG, KENNETH WILKOWSKI, LUIGI G. MARZILLI,* and THOMAS J. KISTENMACHER*

Received October 30, 1980

The preparation and molecular and crystal structure of the complexes (dien)(7,9-dimethylguanine)platinum(II) hexafluorophosphate, $Pt(C_4H_{13}N_3)(C_7H_9N_5O)(PF_6)_2$, and (dien)(7,9-dimethylhypoxanthine)platinum(II) hexafluorophosphate sesquihydrate, $Pt(C_4H_{13}N_3)(C_7H_8N_4O)(PF_6)_2(H_2O)_{1.5}$, are reported (dien = diethylenetriamine). The 7,9-dimethylguanine complex crystallizes in the triclinic system, of space group $P\bar{1}$, with a = 11.111 (3) Å, b = 11.940 (3) Å, c = 9.440 (3) Å, α = 103.54 (2)°, β = 102.39 (2)°, γ = 70.34 (2)°, V = 1133.8 Å^3, Z = 2, D_{measd} = 2.30 (4) g cm^{-3}, and D_{calcd} = 2.24 g cm^{-3}. The 7,9-dimethylhypoxanthine complex crystallizes in the monoclinic system, of space group $C2/c$, with a = 15.754 (5) Å, b = 19.162 (7) Å, c = 18.108 (4) Å, β = 119.02 (2)°, V = 4780.1 Å^3, Z = 8, D_{measd} = 2.137 (3) g cm^{-3}, and D_{calcd} = 2.166 g cm^{-3}. Intensities for 6632 (7,9-dimethylguanine complex) and 4889 (7,9-dimethylhypoxanthine complex) symmetry-averaged reflections were collected in the θ–2θ scan mode on an automated diffractometer employing graphite-monochromatized Mo Kα radiation. Both structures were solved by standard heavy-atom Patterson and Fourier methods. Full-matrix least-squares refinement has led to final R values of 0.049 and 0.057 for the 7,9-dimethylguanine and the 7,9-dimethylhypoxanthine structures, respectively. The primary coordination sphere about the platinum(II) center is approximately square planar in both complex cations, with the tridentate dien chelate, its terminal amino groups in trans positions, and N(1) of the 7,9-dimethylated purine base [Pt–N(1) = 2.044 (5) Å for the guanine base and Pt–N(1) = 2.051 (6) Å for the hypoxanthine base] occupying the four coordination sites. In both complexes, the exocyclic carbonyl oxygen atom O(6) participates in inter- and intracomplex hydrogen-bonding interactions with the amino protons of the dien chelate. For the 7,9-dimethylguanine system, this latter interaction is weak [N(dien)···O(6) = 3.039 (6) Å], but the observed Pt···O(6) intramolecular distance of 3.021 (6) Å suggests some O(6) participation in the metal binding scheme. In contrast, the interligand, intramolecular hydrogen bonding to O(6) in the 7,9-dimethylhypoxanthine complex is stronger [N(dien)···O(6) = 2.946 (6) Å] but there is little indication of O(6) participation [Pt···O(6) = 3.145 (5) Å] in the metal binding. The dihedral angle between the coordination plane and that of the purine base is a sensitive indicator of the relative degree of Pt···O(6) interaction and N(dien)···O(6) interligand hydrogen bonding, and the respective values for this angle for the guanine and hypoxanthine complexes are 62.4 (3) and 47.7 (3)°. The difference in the molecular geometry of the two complex cations can be ascribed to the additional intracomplex steric interactions in the 7,9-dimethylguanine system owing to the presence of the exocyclic amino group at position 2 of the purine ring. Qualitatively, the molecular properties of these N(1)-bound Pt–6-oxopurine complexes are similar to those displayed by N(3)-bound Pt–cytosine complexes. Both crystal structures are characterized by extensive intercomplex hydrogen bonding (direct in the 7,9-dimethylguanine complex and both direct and water mediated in the 7,9-dimethylhypoxanthine complex) and numerous interactions between the PF_6^- anions and the cationic coordination complexes.

Introduction

Since the original report by Rosenberg[2] on the antineoplastic activity of *cis*-$[Pt^{II}(NH_3)_2Cl_2]$, a large body of data have been acquired as to the mode of action of this and similar compounds.[3] Numerous studies have suggested that DNA is the

*To whom correspondence should be addressed at The Johns Hopkins University.

(1) For parts 1 and 2 of this series see: (a) Marzilli, L. G.; Wilkowski, K.; Chiang, C. C.; Kistenmacher, T. J. *J. Am. Chem. Soc.* **1979**, *101*, 7504. (b) Kistenmacher, T. J.; Wilkowski, K.; de Castro, B.; Chiang, C. C.; Marzilli, L. G. *Biochem. Biophys. Res. Commun.* **1979**, *91*, 1521.

0020-1669/81/1320-1835$01.25/0

principal molecular target of these drugs.[4] However, the mechanism of action of the Pt(II) antitumor agents remains quantitatively unknown.

It has been quite convincingly established,[5] however, that the endocyclic nitrogen atoms of the heterocyclic purine and pyrimidine bases are the dominant metal binding sites for Pt(II). Considerable evidence has been accumulated that Pt(II) reagents will attack guanine residues in DNA and that DNA's rich in GC content show preferential binding as evidenced by changes in density centrifugation.[6] Recently, Bauer, Lippard, and their co-workers[7] have provided elegant experimental data for the selective binding of *cis*-$[Pt^{II}(NH_3)_2Cl_2]$ to the $(dG)_n$·$(dC)_n$ ($n \leq 4$) sequence in circular pSM1 DNA at low Pt/P ratios.

The increased speculation that guanine residues in a DNA polymer are a prime target of Pt(II) drugs has led to the proposal of two types of explanations for the mode of action of these reagents. The first type, and perhaps the most attractive, involves the formation of an intrastrand linkage between two guanine bases bound through their endocyclic nitrogen atoms N(7) to a single Pt(II) center.[8-10] Several intrastrand cross-linking models containing Pt(II) and guanosine,[11,12] the dianion of inosine 5′-monophosphate,[13-16] the dianion of guanosine 5′-monophosphate,[17] and the phosphate methyl ester of guanosine 5′-monophosphate are known and have been shown to contain appreciable amounts of intercomplex and intracomplex base–base interactions. An alternative type of explanation involves the formation of an N(7), O(6) chelate between the guanine base and a Pt(II) center.[19] This hypothesis is attractive since, by involving the 6-oxo group in the interaction with the electrophilic Pt(II) center, the chelation model affords a mechanism for base mispairing and thereby an explanation for the effectiveness of the Pt(II) agent.[19] However, no definitive structural evidence exists for such a chelation mode.

Recently, a third type of explanation for the mode of action of Pt(II) agents has evolved. This explanation focuses on the possibility that a Pt–N(1) coordination bond to a 6-oxopurine base concomitant with proton release may play an important role in some aspects of Pt(II)–DNA biochemistry.[20-23] In particular, it has been speculated that Pt(II)–N(1) linkages may act in conjunction with the neighboring O(6) carbonyl oxygen atom either in a multiple metal binding mode similar to that found in α-pyridone blue[21-23] or in a single site N(1), O(6) chelation arrangement.[1a] Such a chelation arrangement has some precedence[1a] and seems geometrically more feasible than an N(7), O(6) arrangement.

Since the available sites on a Pt(II) center can be controlled by the judicious choice of chelate and/or trans effect ligands, considerable insight has been gained from structure–activity relationships for Pt(II) drugs and structure–reactivity relationships for Pt(II)–nucleic acid interactions. This has led to the identification of two broad classes of compounds. In type I systems, there is one reaction site per Pt(II) center [e.g., (dien)$PtCl^+$ (dien = diethylenetriamine)], and in the type II systems there are two reaction sites per Pt(II) center [e.g., *cis*- and *trans*-$[(NH_3)_2PtCl_2]$]. The type I complexes produce only minor modifications in the secondary structure of DNA and have low mutagenicity profiles.[3] For the type II systems, both the cis and trans isomers alter rather dramatically the secondary structure of DNA, but only the cis isomer is highly

Table I. Crystal Data for [(dien)Pt(7,9-Dmgua)]$(PF_6)_2$ and [(dien)Pt(7,9-Dmhyp)]$(PF_6)_2$·$1.5H_2O$

	Dmgua	Dmhyp
a, Å	11.111 (3)	15.754 (5)
b, Å	11.940 (3)	19.162 (7)
c, Å	9.440 (3)	18.108 (4)
α, deg	103.54 (2)	
β, deg	102.39 (2)	119.02 (2)
γ, deg	70.34 (2)	
V, $Å^3$	1133.8	4780.1
space group	$P\bar{1}$	$C2/c$
mol wt	767.4	779.4
D_{measd}, g/cm^3	2.30 (4)	2.137 (3)
D_{calcd}, g/cm^3	2.24	2.166
Z	2	8
formula	$[Pt(C_4H_{13}N_3)(C_7H_9N_5O)]^{2+}(PF_6^-)_2$	$[Pt(C_4H_{13}N_3)(C_7H_8N_4O)]^{2+}(PF_6^-)_2(H_2O)_{1.5}$

Table II. Intensity Collection Data for [(dien)Pt(7,9-Dmgua)]$(PF_6)_2$ and [(dien)Pt(7,9-Dmhyp)]$(PF_6)_2$·$1.5H_2O$

	Dmgua	Dmhyp
cryst dimens,[a] mm	(001)–(00$\bar{1}$), 0.38 (010)–(0$\bar{1}$0), 0.16 ($\bar{1}$00)–($\bar{1}$00), 0.22 (1$\bar{1}$0), 0.10	(001)–(00$\bar{1}$), 0.25 (010)–(0$\bar{1}$0), 0.10 ($\bar{1}$00)–($\bar{1}$00), 0.30
2θ limits, deg	3–60	3–55
scan rate, deg/min	1.5	2–24
total data	13364	12202
R_{av}, %	1.8	4.4
unique data	6666/6632 ($I > 0$)	5734/4889 ($I > \sigma(I)$)
μ[λ(Mo K$\bar{\alpha}$) = 0.710 69 Å], cm^{-1}	67.7	64.4
transmission factor range	0.22–0.39	0.18–0.53

[a] Where two faces are reported, the distance given is the mean separation between them. For one face the value given is the mean distance from the center of the crystal.

(2) Rosenberg, B.; Van Camp, L.; Trosko, J. E.; Mansour, V. H. *Nature (London)* **1969**, *222*, 385.
(3) See: *Biochimie* **1978**, *60*, No. 9.
(4) Roberts, J. J.; Thomson, A. J. *Prog. Nucleic Acid Res. Mol. Biol.* **1979**, *22*, 71.
(5) de Castro, B.; Kistenmacher, T. J.; Marzilli, L. G. "Trace Elements in the Pathogenesis and Treatment of Inflammatory Conditions"; Rainsford, K. D., Brune, K., Whitehouse, M. W., Eds.; Agents and Actions: Basel, 1980.
(6) Stone, P. J.; Kelman, A. J.; Sinex, F. M. *Nature (London)* **1974**, *251*, 736.
(7) Cohen, G. L.; Ledner, J. A.; Bauer, W. R.; Ushay, H. M.; Caravana, C.; Lippard, S. *J. Am. Chem. Soc.* **1980**, *102*, 2487.
(8) Marzilli, L. G. *Prog. Inorg. Chem.* **1977**, *23*, 255.
(9) Kelman, A. D.; Buchbinder, M. *Biochimie* **1978**, *60*, 893.
(10) Marzilli, L. G.; Kistenmacher, T. J.; Eichhorn, G. L. In "Nucleic Acid-Metal Interactions"; Spiro, T. G., Ed.; Wiley: New York, 1980; Chapter 5.
(11) Gellert, R. W.; Bau, R. *J. Am. Chem. Soc.* **1975**, *97*, 7379.
(12) Cramer, R. E.; Dahlstrom, P. L. *J. Clin. Hematol. Oncol.* **1977**, *7*, 330. Cramer, R. E.; Dahlstrom, P. L.; Seu, M. J. T.; Norton, T.; Kashiwagi, M. *Inorg. Chem.* **1980**, *19*, 148.
(13) Goodgame, D. M. L.; Jeeves, I.; Phillips, F. L.; Skapski, A. C. *Biochim. Biophys. Acta* **1975**, *378*, 153.
(14) Bau, R.; Gellert, R. W.; Lehovec, S. M.; Louie, S. *J. Clin. Hematol. Oncol.* **1977**, *7*, 51.
(15) Kistenmacher, T. J.; Chiang, C. C.; Chalilpoyil, P.; Marzilli, L. G. *Biochem. Biophys. Res. Commun.* **1978**, *84*, 70.
(16) Kistenmacher, T. J.; Chiang, C. C.; Chalilpoyil, P.; Marzilli, L. G. *J. Am. Chem. Soc.* **1979**, *101*, 1143.
(17) Bau, R.; Gellert, R. W. *Biochimie* **1978**, *60*, 1040.
(18) Marzilli, L. G.; Chalilpoyil, P.; Chiang, C. C.; Kistenmacher, T. J. *J. Am. Chem. Soc.* **1980**, *102*, 2480.
(19) Rosenberg, B. *Biochimie* **1978**, *60*, 859.
(20) Chu, G. Y. H.; Mansy, S.; Duncan, R. E.; Tobias, R. S. *J. Am. Chem. Soc.* **1978**, *100*, 593.
(21) Barton, J. K.; Lippard, S. J. *Ann. N.Y. Acad. Sci.* **1978**, *313*, 686.
(22) Barton, J. K.; Szalda, D. J.; Rabinowitz, H. N.; Waszczak, J. V.; Lippard, S. J. *J. Am. Chem. Soc.* **1979**, *101*, 1434.
(23) Barton, J. K.; Lippard, S. J. In "Nucleic Acid-Metal Interactions"; Spiro, T. G., Ed.; Wiley: New York, 1980; Chapter 2.

Table III. Final Nonhydrogen Atom Coordinates for [(dien)Pt(7,9-Dmgua)]$(PF_6)_2$[a]

atom	x	y	z	atom	x	y	z
Pt[b]	27738 (2)	2391 (2)	36364 (2)	C(11)	3207 (7)	−2221 (6)	2352 (9)
O(6)	3464 (4)	2269 (4)	5893 (5)	C(12)	4446 (7)	−1088 (6)	1543 (7)
N(1)	1623 (4)	1864 (4)	4561 (5)	C(13)	4867 (6)	13 (6)	2140 (7)
N(2)	−248 (5)	1503 (5)	3144 (6)	P(1)	1014 (2)	1609 (1)	9056 (2)
N(3)	−508 (4)	3224 (4)	4892 (5)	P(2)	5461 (2)	3304 (2)	2446 (2)
N(7)	1632 (5)	4475 (4)	7602 (5)	F(11)	800 (6)	1231 (5)	7313 (5)
N(9)	−453 (5)	4880 (4)	6939 (6)	F(12)	−145 (6)	1139 (7)	9075 (7)
N(10)	1925 (5)	838 (5)	4233 (6)	F(13)	1918 (7)	344 (5)	9235 (8)
N(11)	3945 (5)	−1346 (4)	2721 (6)	F(14)	2164 (7)	2039 (9)	8967 (8)
N(13)	3764 (5)	990 (4)	2744 (5)	F(15)	69 (7)	2889 (5)	8857 (7)
C(2)	294 (5)	2248 (5)	4232 (6)	F(16)	1192 (6)	2010 (5)	10817 (5)
C(4)	116 (5)	3857 (5)	5984 (6)	F(21)	6384 (5)	1980 (5)	2682 (8)
C(5)	1434 (5)	3601 (5)	6410 (6)	F(22)	4415 (5)	2715 (5)	1383 (5)
C(6)	2273 (5)	2567 (5)	5654 (6)	F(23)	6100 (6)	3221 (6)	1060 (6)
C(7)	2888 (8)	4519 (7)	8481 (8)	F(24)	4789 (5)	3358 (5)	3802 (5)
C(8)	481 (7)	5215 (5)	7892 (7)	F(25)	6482 (5)	3874 (5)	3514 (6)
C(9)	−1852 (8)	5425 (7)	6917 (10)	F(26)	4549 (5)	4601 (5)	2211 (6)
C(10)	2625 (7)	−2138 (6)	3668 (10)				

[a] Estimated standard deviations in the least significant figure are enclosed in parentheses in this and in all the following tables. [b] Parameters × 10^5; for all other atoms, parameters × 10^4.

mutagenic.[3] In this same vein, only the cis isomers of type II complexes are active antineoplastic agents.[3] Presently, there are several structurally characterized models for both the type I and II systems for N(7)-bound Pt(II) complexes.[5,10]

Given the recent interest in the possible role of N(1)–Pt(II) binding in DNA biochemistry for 6-oxopurine bases,[1,21-23] we have undertaken a series of synthetic, spectroscopic, and structural studies of Pt(II)–N(1)-bound 6-oxopurine complexes of both type I and type II.[1] We describe herein the preparation and molecular and crystal structure of two N(1)-bound type I complexes containing the modified purine base 7,9-dimethylguanine (7,9-Dmgua) and 7,9-dimethylhypoxanthine (7,9-Dmhyp).

Experimental Section

A. [(dien)(7,9-Dmgua)Pt^{II}]$(PF_6)_2$. (a) Synthesis. A suspension of Pt(dien)I_2[24] (0.400 g) in 15 mL of H_2O was added to 5 mL of an aqueous solution of $AgNO_3$ (0.246 g). The mixture was warmed to 60 °C and maintained at this temperature with stirring for 2 h. After the mixture was cooled, solid AgI was removed by filtration, and 7,9-Dmgua[25] (0.130 g) was added to the filtrate. After being heated, the solution was filtered, and to it was added 0.236 g of NH_4PF_6. The resulting solution was then set aside for slow evaporation at ambient temperature. Colorless, well-formed and multifaceted, crystals were obtained after a few days.

(b) Collection and Reduction of the X-ray Intensity Data. Preliminary oscillation and Weissenberg photographs showed the crystal system to be triclinic. Unit cell dimensions and their associated standard deviations were derived from a least-squares fit to the setting angles for 15 carefully selected and centered reflections on a Syntex $P\bar{1}$ automated diffractometer. The crystal density, measured by the neutral buoyancy method in a mixture of carbon tetrachloride and bromoform, indicated 2 formula units per cell. Complete crystal data are collected in Table I.

The intensities of 13 364 reflections (the full sphere to $2\theta = 60°$) were measured on the diffractometer employing graphite-monochromatized Mo K$\bar{\alpha}$ radiation. The crystal used in data collection was mounted approximately parallel to the crystallographic c axis, and its dimensions and face assignments are reported in Table II. Intensity data were collected in the θ–2θ scan mode with a constant scan speed (in 2θ) of 1.5°/min. Pertinent data collection parameters are also given in Table II. The intensities of three standards were monitored after every 97 reflections and showed no systematic variation over the course of the experiment. The measured intensities were symmetry averaged and reduced to a set of 6666 independent values; of these 6632 had net intensities above zero and were assigned observational variances on the basis of the equation $\sigma^2(I) = S + (B_1 + B_2)(T_S/2T_B)^2 + (pI)^2$, where S, B_1, and B_2 are the scan and extremum background counts, T_S and T_B are the scan and individual background counting times ($T_B = T_S/4$ for all reflections), and p was taken to be 0.03 and represents an estimate of the error[26] proportional to the diffracted intensity. Reflections with negative net intensities were assigned F's and weights equal to zero. The positive net intensities and their estimated standard deviations were corrected for Lorentz and polarization effects. An absorption correction was also applied on the basis of the dimensions and face assignments given in Table II. An approximation to the absolute scale factor was derived by the method of Wilson.[27]

(c) Solution and Refinement of the Structure. The positional coordinates of the Pt atom and those of the 6-oxopurine base were deduced from a three-dimensional Patterson synthesis. A subsequent structure factor–Fourier calculation allowed the positions of the remaining nonhydrogen atoms in the asymmetric unit to be obtained. Several cycles of isotropic refinement, minimizing the quantity of $\sum w(|F_o| - |F_c|)^2$ where $w = 4F_o^2/\sigma^2(F_o^2)$, led to an R value $[\sum||F_o| - |F_c||/\sum|F_o|]$ of 0.10. Two further cycles, employing anisotropic thermal parameters for the nonhydrogen atoms, reduced the R value to 0.058. A subsequent difference-Fourier synthesis allowed the positioning of the 22 independent hydrogen atoms; the temperature factors of the hydrogen atoms were fixed at about the value for the atom to which they were attached plus 1.0 Å^2. Finally, two cycles of anisotropic refinement were performed, holding the hydrogen atom parameters fixed and led to convergence (maximum shift/error for any parameter of 0.46) and a final R value of 0.057. The final weighted R value $\{[\sum w(|F_o| - |F_c|)^2/\sum w|F_o|^2]^{1/2}\}$ and goodness of fit $\{[\sum w(|F_o| - |F_c|)^2/(NO - NV)]^{1/2}$, where NO = 6630 reflection data and NV = 316 variables$\}$ were 0.053 and 3.0, respectively. In these final cycles of refinement the weights of the 010 and the 100 reflections were set equal to zero as their experimental diffraction profiles were obviously and severely affected by the presence of the diffracted beam stop. A final difference-Fourier synthesis was essentially featureless (maximum and minimum peaks less than ±0.5 e/Å^3), with the exception of a peak at ~4 e/Å^3 near the Pt site.

Neutral scattering factor curves for the nonhydrogen[28] and hydrogen[29] atoms were taken from common sources. Anomalous dispersion corrections were applied to the scattering curves for all nonhydrogen atoms.[30] Final atomic positional parameters for the nonhydrogen atoms are collected in Table III. Tables of anisotropic thermal parameters, parameters for the hydrogen atoms, and final calculated and observed structure factor amplitudes are available as supplementary material.[31]

(24) Mann, F. G. *J. Chem. Soc.* **1934**, 466.
(25) Jones, J.; Robins, R. *J. Am. Chem. Soc.* **1962**, *34*, 1914.
(26) Busing, W. R.; Levy, H. A. *J. Chem. Phys.* **1957**, *26*, 563.
(27) Wilson, A. J. C. *Nature (London)* **1942**, *150*, 152.
(28) Hanson, H. P.; Herman, F.; Lea, J. D.; Skillman, S. *Acta Crystallogr.* **1964**, *17*, 1040.
(29) Stewart, R. F.; Davidson, E. R.; Simpson, W. T. *J. Chem. Phys.* **1965**, *42*, 3175.
(30) Cromer, D. T.; Liberman, D. *J. Chem. Phys.* **1970**, *53*, 1891.

Table IV. Final nonhydrogen Atom Coordinates for [(dien)Pt(7,9-Dmhyp)]$(PF_6)_2 \cdot 1.5H_2O$

atom	x	y	z	atom	x	y	z
Pt[a]	11 (2)	12227 (2)	46404 (2)	C(13)	−232 (6)	1105 (5)	6120 (5)
O(6)	1755 (4)	179 (3)	5503 (3)	P(1)	0[b]	3139 (1)	2500[b]
N(1)	1331 (4)	1172 (3)	4695 (3)	P(2)	5000[b]	1944 (2)	2500[b]
N(3)	2423 (4)	1775 (4)	4343 (4)	P(3)	2450 (2)	4519 (2)	1672 (2)
N(7)	3761 (4)	390 (3)	5884 (4)	F(11)	0[b]	3962 (4)	2500[b]
N(9)	4040 (4)	1245 (4)	5014 (4)	F(12)	0[b]	2323 (5)	2500[b]
N(10)	−825 (5)	1401 (4)	3369 (4)	F(13)	1011 (4)	3147 (4)	3322 (4)
N(11)	−1263 (4)	1299 (3)	4641 (4)	F(14)	521 (7)	3120 (4)	1941 (4)
N(13)	578 (4)	1131 (3)	5917 (4)	F(21)	4346 (5)	1924 (4)	1487 (3)
C(2)	1590 (5)	1687 (4)	4332 (5)	F(22)	4310 (5)	2523 (3)	2539 (6)
C(4)	3061 (5)	1290 (4)	4839 (4)	F(23)	4309 (4)	1360 (3)	2543 (3)
C(5)	2912 (5)	764 (4)	5249 (4)	F(31)	3057 (6)	4900 (8)	1395 (7)
C(6)	1987 (5)	651 (4)	5183 (4)	F(32)	3224 (8)	3933 (5)	1973 (5)
C(7)	3928 (7)	−208 (5)	6240 (6)	F(33)	3102 (9)	4778 (5)	2587 (5)
C(8)	4438 (6)	704 (5)	5534 (5)	F(34)	1882 (9)	4119 (10)	1954 (10)
C(9)	4534 (7)	1704 (6)	4705 (6)	F(35)	1706 (10)	5090 (6)	1370 (6)
C(10)	−1856 (7)	1430 (6)	3147 (5)	F(36)	1894 (12)	4320 (7)	774 (5)
C(11)	−1934 (6)	1718 (5)	3907 (5)	W(1)	2851 (5)	2872 (4)	3369 (4)
C(12)	−1059 (6)	1542 (5)	5486 (5)	W(2)	0[b]	486 (5)	2500[b]

[a] Parameters × 10^5; for all other atoms, parameters × 10^4. [b] Parameters fixed by symmetry.

B. [(dien)(7,9-Dmhyp)Pt^{II}]$(PF_6)_2 \cdot 1.5H_2O$. (a) Synthesis. The method used for the preparation of the 7,9-Dmhyp complex was essentially identical with the one described above for the 7,9-Dmgua derivative, the only difference being that the solution containing the nitrate salt of the complex was allowed to evaporate to near dryness, filtered, and then redissolved (0.330 g) in H_2O prior to the addition of KPF_6 (0.207 g). After slow evaporation at room temperature, colorless, crystalline parallelepipeds were collected.

(b) Collection and Reduction of the X-ray Intensity Data. The crystal system (monoclinic) and the space group ($C2/c$; systematic absences hkl, $h + k = 2n + 1$, and $h0l$, $l = 2n + 1$) were determined from preliminary oscillation, Weissenberg, and precession photographs. The experimental techniques described above for the data collection and reduction of intensity data were also used for this crystal. Crystal data and relevant data collection parameters are collected in Tables I and II, respectively.

(c) Solution and Refinement of the Structure. A structural solution was readily formulated from standard Patterson–Fourier techniques. Several cycles of isotropic refinement led to an R value of 0.10. Two further cycles, employing anisotropic thermal parameters for the nonhydrogen atoms, reduced the R values to 0.07. A difference-Fourier synthesis allowed the positioning of the 24 hydrogen atoms. Two subsequent cycles of refinement, holding the hydrogen atom parameters fixed [$B_H(\text{iso}) = B_{C,N,O} + 1.5$ Å^2], led to convergence (maximum shift/error for any parameter of 0.8) and a final R value of 0.057. The final weighted R value and goodness of fit (with NO = 4889 reflection data and NV = 323 variables) were 0.051 and 1.92, respectively. A final difference-Fourier map showed a peak in the difference density at about 1.4 e/Å^3 near the Pt atom, but otherwise no feature exceeded ±0.6 e/Å^3.

Anomalous dispersion corrections[30] were applied to the scattering curves[28] for all nonhydrogen atoms. The uncorrected hydrogen atom scattering curves were as above.[29] Final atomic positional parameters for the nonhydrogen atoms are given in Table IV. Tables of anisotropic thermal parameters, parameters for the hydrogen atoms, and final calculated and observed structure factor amplitudes are available as supplementary material.[31]

The crystallographic calculations were performed for both analyses with a standard set of computer programs.[32]

Results and Discussion

The dimethylated purine bases 7,9-Dmgua and 7,9-Dmhyp (Figure 1) are well suited[1] for the preparation of N(1)-bound metal compounds as the common N(7) coordination site is blocked and the N(1) site is deprotonated and has a lone pair of electrons available for metal coordination. We have been able to prepare both type I and type II Pt(II) complexes containing these modified purine ligands,[1b] and we describe in detail here the preparation and molecular and crystal structure of two type I complexes, [(dien)(7,9-Dmgua)Pt^{II}-$(PF_6)_2$ (Figures 2–4) and [(dien)(7,9-Dmhyp)Pt^{II}]$(PF_6)_2 \cdot 1.5H_2O$[1b] (Figures 5–8), and compare the results obtained for these N(1)-bound complexes to the more common N(7)-bound species.

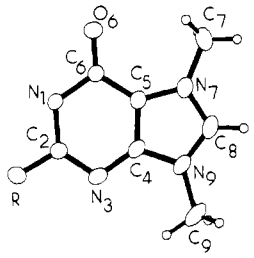

Figure 1. Molecular structure and atomic numbering scheme for the two alkylated purine bases 7,9-dimethylhypoxanthine (7,9-Dmhyp) (R = H) and 7,9-dimethylguanine (7,9-Dmgua) (R = NH_2).

X-Ray Structural Characterization of the Metal Coordination Geometry. The molecular conformations of the [(dien)(7,9-Dmgua)Pt^{II}]$^{2+}$ and [(dien)(7,9-Dmhyp)Pt^{II}]$^{2+}$ cations are illustrated in the stereoviews of Figures 2 and 5, respectively. Details of their molecular geometries are presented in Tables V–VII. Each cation exhibits a slightly distorted square-planar geometry with the four equatorial coordination sites occupied by the tridentate dien chelate, its terminal amino groups in trans positions, and the endocyclic nitrogen atom N(1) of the 7,9-Dmgua, (Figure 2) or the 7,9-Dmhyp (Figure 5) purine base.

We will compare in detail some aspects of these N(1)-bound type I complexes with those found for the analogous N(7)-bound type I complexes[33] [(dien)(guanosine)Pt^{II}]$(ClO_4)_2$[34] and [(dien)(inosine)Pt^{II}]$(NO_3)_2$,[35] where hypoxanthine is the purine base of the nucleoside inosine. The Pt(II)–N(1) bond lengths of 2.044 (5) (7,9-Dmgua) and 2.051 (6) Å (7,9-Dmhyp) are systematically ~0.02 Å longer than for the N(7)-bound guanosine and inosine complexes, 2.035 (13)[34] and 2.029 (9) Å,[35] respectively. This slight elongation of the Pt(II)–N(base) bond length for the N(1)-bound complexes does not necessarily

(31) See paragraph at end of the paper regarding supplementary material.
(32) Crystallographic programs employed include Wehe, Busing, and Levy's ORABS, Zalkin's FORDAP, Busing, Martin, and Levy's ORFLS (modified), Pippy and Ahmed's MEAN PLANE, Johnson's ORTEP, and Gantzel and Trueblood's MGTLS.

(33) Macquet, J. P.; Butour, J. L. *Biochimie* **1978**, *60*, 901.
(34) Melanson, R.; Rochon, F. D. *Can. J. Chem.* **1979**, *57*, 57.
(35) Melanson, R.; Rochon, F. D. *Acta Crystallogr., Sect. B* **1978**, *B34*, 3594.

Table V. Molecular Geometry for the $[(dien)Pt(7,9\text{-}Dmgua)]^{2+}$ and the $[(dien)Pt(7,9\text{-}Dmhyp)]^{2+}$ Cations

bond length, Å, or angle, deg	7,9-Dmgua	7,9-Dmhyp
(a) Primary Coordination Sphere about the Pt Atom		
Pt-N(1)	2.044 (5)	2.051 (6)
Pt-N(10)	2.060 (6)	2.051 (7)
Pt-N(11)	2.020 (6)	1.998 (7)
Pt-N(13)	2.034 (5)	2.041 (7)
N(1)-Pt-N(10)	97.2 (2)	98.0 (3)
N(1)-Pt-N(11)	178.5 (2)	177.2 (3)
N(1)-Pt-N(13)	94.2 (2)	93.3 (3)
N(10)-Pt-N(11)	84.2 (2)	84.2 (3)
N(10)-Pt-N(13)	168.1 (2)	168.0 (3)
N(11)-Pt-N(13)	84.4 (2)	84.4 (3)
(b) dien Chelate		
N(10)-C(10)	1.51 (1)	1.47 (1)
C(10)-C(11)	1.49 (1)	1.54 (1)
C(11)-N(11)	1.47 (1)	1.47 (1)
N(11)-C(12)	1.48 (1)	1.48 (1)
C(12)-C(13)	1.49 (1)	1.51 (1)
C(13)-N(13)	1.49 (1)	1.49 (1)
Pt-N(10)-C(10)	108.0 (4)	109.1 (6)
N(10)-C(10)-C(11)	110.1 (6)	109.0 (8)
C(10)-C(11)-N(11)	108.0 (6)	106.1 (7)
Pt-N(11)-C(11)	106.7 (4)	108.6 (5)
Pt-N(11)-C(12)	106.9 (4)	107.9 (5)
C(11)-N(11)-C(12)	119.5 (5)	117.6 (7)
N(11)-C(12)-C(13)	108.0 (5)	106.7 (7)
C(12)-C(13)-N(13)	108.0 (6)	108.9 (7)
Pt-N(13)-C(13)	108.6 (4)	108.5 (5)
(c) Purine Ligands		
N(1)-C(2)	1.38 (1)	1.36 (1)
N(1)-C(6)	1.40 (1)	1.40 (1)
N(3)-C(2)	1.32 (1)	1.31 (1)
N(3)-C(4)	1.34 (1)	1.34 (1)
N(7)-C(5)	1.38 (1)	1.38 (1)
N(7)-C(7)	1.47 (1)	1.46 (1)
N(7)-C(8)	1.33 (1)	1.36 (1)
N(9)-C(4)	1.38 (1)	1.42 (1)
N(9)-C(8)	1.33 (1)	1.34 (1)
N(9)-C(9)	1.47 (1)	1.47 (1)
O(6)-C(6)	1.23 (1)	1.22 (1)
C(4)-C(5)	1.38 (1)	1.34 (1)
C(5)-C(6)	1.42 (1)	1.42 (1)
N(2)-C(2)	1.37 (1)	
Pt-N(1)-C(2)	124.2 (4)	118.9 (5)
Pt-N(1)-C(6)	115.2 (4)	119.3 (5)
C(2)-N(1)-C(6)	120.5 (5)	121.5 (7)
C(2)-N(3)-C(4)	112.0 (5)	109.4 (7)
C(5)-N(7)-C(7)	126.1 (5)	127.0 (7)
C(5)-N(7)-C(8)	107.8 (5)	107.1 (7)
C(7)-N(7)-C(8)	125.9 (6)	125.9 (7)
C(4)-N(9)-C(8)	107.9 (5)	107.0 (7)
C(4)-N(9)-C(9)	124.5 (6)	127.5 (7)
C(8)-N(9)-C(9)	127.5 (6)	125.5 (8)
N(1)-C(2)-N(3)	127.1 (5)	128.3 (8)
N(3)-C(4)-N(9)	126.0 (5)	124.9 (7)
N(3)-C(4)-C(5)	127.3 (5)	128.0 (7)
N(9)-C(4)-C(5)	106.7 (5)	107.1 (7)
N(7)-C(5)-C(4)	107.1 (5)	109.0 (7)
N(7)-C(5)-C(6)	133.4 (5)	129.9 (7)
C(4)-C(5)-C(6)	119.5 (5)	121.1 (7)
O(6)-C(6)-N(1)	120.9 (5)	121.9 (7)
O(6)-C(6)-C(5)	125.6 (5)	127.1 (7)
N(1)-C(6)-C(5)	113.5 (5)	111.0 (6)
N(7)-C(8)-N(9)	110.5 (6)	109.8 (7)
N(1)-C(2)-N(2)	116.1 (5)	
N(3)-C(2)-N(2)	127.1 (5)	

imply a weaker Pt–base primary interaction in the N(1)-bound complexes, since alkylation at N(7) of the imidazole ring of the 6-oxopurine base in conjunction with deprotonation at N(1) is expected to induce a significant increase in electron density in the pyrimidine ring.[1] These N(1)-bound purine complexes

Table VI. Least-Squares Planes and the Deviation (Å) of Individual Atoms from These Planes for the $[(dien)Pt(7,9\text{-}Dmgua)]^{2+}$ Cation[a]

(a) Primary Coordination Sphere

$-0.5028X + 0.1759Y - 0.8463Z = -4.0550$

Pt	−0.022	N(10)	0.041
N(1)	−0.027	N(11)	−0.035
		N(13)	0.042

(b) Imidazole Ring

$0.3773X + 0.6938Y - 0.6134Z = -0.8225$

N(9)	0.003	C(8)	−0.005
N(7)	0.005	C(7)	−0.083*
C(4)	0.001	C(9)	0.001*
C(5)	−0.003		

(c) Pyrimidine Ring

$0.3839X + 0.6499Y - 0.6560Z = -1.1869$

N(1)	−0.024	C(5)	−0.008
N(3)	0.013	C(6)	0.024
C(2)	0.005	O(6)	0.083*
C(4)	−0.012	N(2)	−0.038*

(d) 7,9-Dimethylguanine Ligand

$0.3820X + 0.6707Y - 0.6357Z = -1.0500$

N(1)	−0.051	C(6)	0.028
N(3)	0.025	C(8)	−0.038
N(7)	0.000	Pt	−0.331*
N(9)	−0.011	O(6)	0.081*
C(2)	−0.016	N(2)	−0.092*
C(4)	0.031	C(7)	−0.098*
C(5)	0.033	C(9)	−0.094*

[a] In each of the equations of the planes, X, Y, and Z are coordinates referred to the orthogonal axes X along the a axis, Y in the ab plane, and Z along the c^* axis. Atoms designated by an asterisk were given zero weight in calculating the planes; the atoms used to define the planes were given equal weight.

Table VII. Least-Squares Planes and the Deviation (Å) of Individual Atoms from These Planes for the $[(dien)Pt(7,9\text{-}Dmhyp)]^{2+}$ Cation[a]

(a) Primary Coordination Sphere

$-0.0585X - 0.9901Y - 0.1275Z = -3.0591$

Pt	0.041	N(10)	−0.030
N(1)	0.007	N(11)	0.013
		N(13)	−0.030

(b) Imidazole Ring

$0.1308X - 0.5940Y - 0.7938Z = -7.4707$

N(7)	0.004	C(8)	−0.008
N(9)	0.008	C(7)	−0.043*
C(4)	−0.005	C(9)	−0.005*
C(5)	0.001		

(c) Pyrimidine Ring

$0.1206X - 0.5774Y - 0.8075Z = -7.5415$

N(1)	−0.003	C(5)	−0.018
N(3)	0.025	C(6)	0.022
C(2)	−0.021	O(6)	0.057*
C(4)	−0.004		

(d) 7,9-Dimethylhypoxanthine Ligand

$0.1280X - 0.5842Y - 0.8014Z = -7.5194$

N(1)	−0.010	C(6)	0.031
N(3)	0.021	C(8)	−0.019
N(7)	−0.011	Pt	−0.260*
N(9)	0.014	O(6)	0.071*
C(2)	−0.033	C(7)	−0.076*
C(4)	0.008	C(9)	0.028*
C(5)	0.000		

[a] In each of the equations of the planes, X, Y, and Z are coordinates referred to the orthogonal axes a, b, and c^*. Atoms designated by an asterisk were given zero weight in calculating the planes; the atoms used to define the planes were given equal weight.

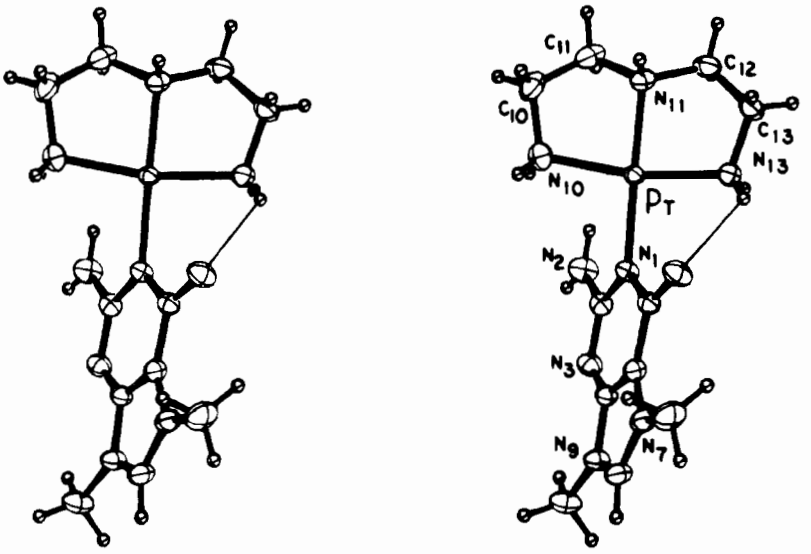

Figure 2. Stereoview of the molecular structure of the $[(dien)Pt(7,9\text{-}Dmgua)]^{2+}$ cation. The thin line denotes the weak interligand hydrogen bond.

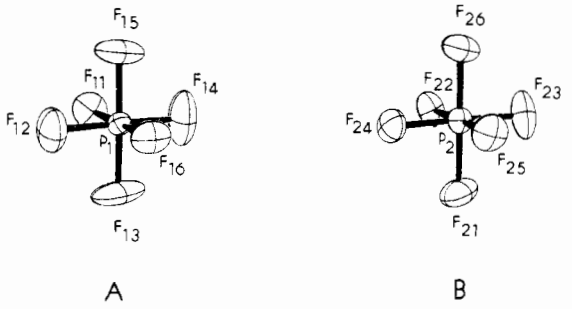

Figure 3. Perspective views of the two independent hexafluorophosphate anions in the $[(dien)Pt(7,9\text{-}Dmgua)](PF_6)_2$ structure.

show metal–ligand distances more typical[5,10] of metal–pyrimidine complexes than of the more common N(7)-bound metal–purine complexes.

In addition to the primary metal–base linkage, two types of secondary interactions in metal–6-oxopurine complexes have received considerable attention: (1) interligand hydrogen bonding involving O(6) of the purine base and other ligands in the primary metal coordination sphere;[36-38] (2) possible metal···O(6) interaction leading to a chelation mode.[5,10,36-38] Interligand hydrogen bonding utilizing one of the terminal amino groups of the dien chelate as the donor and O(6) of the N(7)-bound 6-oxopurine base as the acceptor has been noted to be weak in the guanosine complex [N(dien)···O(6) = 3.18 (2) Å][34] and possibly to be considerably stronger in the inosine complex [N(dien)···O(6) = 2.87 (1) Å].[35] The opposite situation obtains here in the N(1)-bound complexes, with a relatively strong interligand hydrogen bond in the 7,9-Dmhyp complex [N(dien)···O(6) = 2.946 (6) Å (Table VIII)] and a weaker interaction in the 7,9-Dmgua complex [N(dien)···O(6) = 3.021 (6) Å (Table VIII)]. The difference in the apparent strength of the interligand hydrogen bonding in the N(7)-bound guanosine and inosine complexes may result from a competition between the relatively weak interligand hydrogen bonding and other forces operative in their crystalline structures. We wish to propose an intramolecular basis for the difference in the N(1)-bound compounds studied here.

Table VIII. Distances (Å) and Angles (Deg) in the Intermolecular Interactions of the Type D–H ···A

D	H	D–H	A	H···A	D···A	D–H···A
(a) $[(dien)Pt(7,9\text{-}Dmgua)](PF_6)_2$[a]						
N(10)	H(N10A)	0.89	F(11)^{i}	2.39	3.202 (8)	152
N(11)	H(N11)	0.87	O(6)^{ii}	2.02	2.855 (6)	161
N(13)	H(N13A)	0.88	F(16)^{iii}	2.29	3.072 (7)	148
N(13)	N(13B)	0.87	O(6)	2.45	3.039 (6)	126*[c]
(b) $[(dien)Pt(7,9\text{-}Dmhyp)](PF_6)_2 \cdot 1.5H_2O$[b]						
N(10)	H(N10A)	0.87	W(2)	2.22	3.037 (6)	156
N(10)	H(N10B)	0.89	F(12)	2.28	3.045 (6)	144
N(11)	H(N11)	0.86	O(6)^{iv}	2.09	2.914 (4)	160
N(13)	H(N13A)	0.86	W(1)^{v}	2.07	2.888 (5)	159
N(13)	H(N13B)	0.87	O(6)	2.32	2.946 (6)	129*
N(13)	H(N13B)	0.87	F(33)^{v}	2.36	3.038 (6)	135
W(1)	H(W1A)	1.08	N(3)	1.95	3.023 (6)	172
W(1)	H(W1B)	1.04	F(13)	2.16	2.915 (7)	128
W(2)	H(W2)	1.09	F(31)^{vi}	1.99	2.948 (6)	145

[a] Symmetry transforms (space group $P\bar{1}$): (i) $-x, -y, -1-z$; (ii) $1-x, -y, 1-z$; (iii) $x, y, -1+z$. [b] Symmetry transforms (space group $C2/c$): (iv) $-x, -y, 1-z$; (v) $^1/_2 - x, ^1/_2 - y, 1-z$; (vi) $-^1/_2 + x, -^1/_2 + y, z$. [c] An asterisk indicates intracomplex hydrogen bonds.

The principal difference in the molecular structures of the 7,9-Dmgua and 7,9-Dmhyp bases (and for that matter the nucleosides guanosine and inosine) is the presence of the exocyclic amino group at position 2 of the purine ring in the 7,9-Dmgua base (Figure 1). For the N(7)-bound guanosine and inosine complexes, the exocyclic amino group in the guanosine system has little apparent effect on the electronic or steric properties of these complexes as the additional functional group is far removed from the metal binding site. This is in clear contrast to the N(1)-bound 7,9-Dmgua and 7,9-Dmhyp complexes where the exocylic amino group is appended to one of the carbon atoms α to the metal binding site. The electronic consequences for the metal–ligand binding are difficult to appraise; contrastingly, the steric influence of the exocylic amino group is quite dramatic. A particularly sensitive parameter is the dihedral angle between the coordination plane and that of the purine base which is 47.7 (3)° for the 7,9-Dmhyp complex cation but is strikingly larger at 62.4 (3)° in the 7,9-Dmgua complex cation. From a study of CPK molecular models, it is apparent that the opening of the dihedral angle for the 7,9-Dmgua complex serves to relieve repulsive steric stress between the Pt–dien moiety and the

(36) Marzilli, L. G.; Kistenmacher, T. J. *Acc. Chem. Res.* **1977**, *10*, 146.
(37) Gellert, R. W.; Bau, R. *Met. Ions Bioorg. Systems* **1979**, *8*, 1.
(38) Swaminathan, V.; Sundaralingam, M. *CRC Crit. Rev. Biochem.* **1979**, *6*, 245.

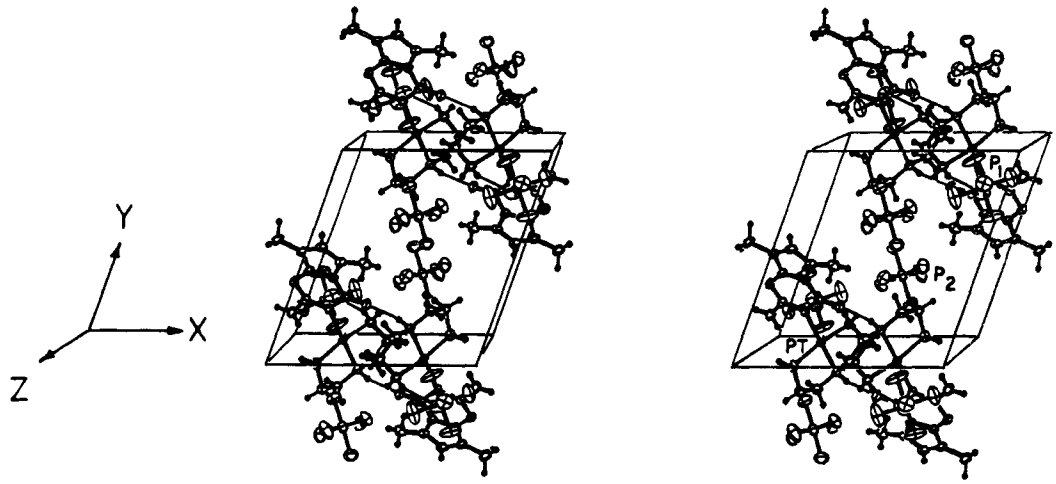

Figure 4. Stereoview of the unit-cell packing of $[(dien)Pt(7,9\text{-}Dmgua)](PF_6)_2$. The thin lines illustrate the intermolecular hydrogen bonding.

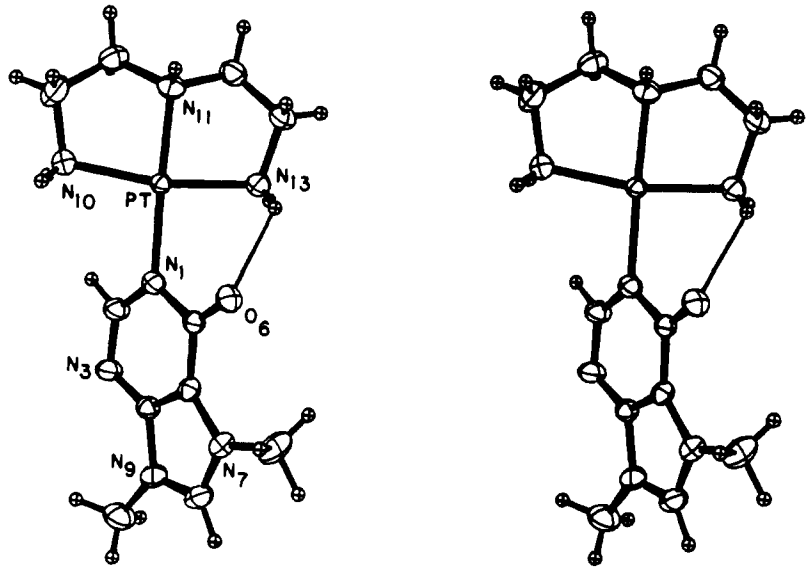

Figure 5. Stereoview of the molecular structure of the $[(dien)Pt(7,9\text{-}Dmhyp)]^{2+}$ cation. The thin line denotes the interligand hydrogen bond.

exocylic amino group on the base.

In addition to this increase in dihedral angle, the consequences of the relief of the steric repulsion in the 7,9-Dmgua complex are threefold: (1) As alluded to above, the interligand hydrogen bonding is measurably reduced in the 7,9-Dmgua complex relative to the 7,9-Dmhyp complex. (2) In conjunction with the opening of the dihedral angle, the 7,9-Dmgua base tilts toward the coordination plane such that the exocyclic angles at N(1) in its complex are now dissymmetric, 124.4 (4) [Pt–N(1)–C(2)] and 115.2 (4)° [Pt–N(1)–O(6)] in contrast to the nearly symmetric values 118.9 (5) and 119.3 (5)°, observed in the 7,9-Dmhyp complex. (3) Finally, there is a measurable reduction in the Pt···O(6) distance in the 7,9-Dmgua complex [3.031 (6) Å] relative to that found in the 7,9-Dmhyp complex [3.145 (6) Å]. Given the near equivalence of the pyrimidine ring in the neighborhood of the metal binding site in 7,9-Dmgua and cytosine, the value for the Pt···O(6) distance in the 7,9-Dmgua complex is expectedly close to the Pt···O(2) distances observed in several Pt(II) and Pd(II) complexes with cytosine derivatives (3.01–3.06 Å).[39-42] In marked contrast, the Pt···O(6) distances are dramatically longer (~3.4 Å) for the Pt–N(7)-bound guanosine and inosine systems.[34,35] Thus, it is clear that Pt–N(3)-bound cytosine and Pt–N(1)-bound 6-oxopurine complexes yield considerably enhanced Pt···O intracomplex interactions over those found in Pt–N(7)-bound 6-oxopurine systems. It should be noted, however, that these "short" Pt···O interaction distances are still well in excess of those (2.7–2.8 Å) found in several Cu(II)–N(3)-bound cytosine[5,36] complexes and in a Cu(II)–N(1)-bound 6-oxopurine complex,[1a] whereas the metal–N distances are only ~0.07 Å longer for Pt.

Last, we note that the $[(dien)(7,9\text{-}Dmgua)Pt^{II}]^{2+}$ and $[(dien)(7,9\text{-}Dmhyp)Pt^{II}]^{2+}$ complex cations are, as a result of the relationship of the purine ligand to the coordination plane, chiral at the Pt(II) center. In the crystalline structure of each complex, there are equal numbers of enantiomers present and related through the $\bar{1}$ symmetry operation common to both centrosymmetric space groups ($P\bar{1}$ and $C2/c$) which describe the symmetry of their crystalline motifs. In fact, for the 7,9-Dmgua complex, the enantiomer of that described in Table III is shown in Figure 2 in order to exhibit the same isomer as described in Table IV and shown in Figure 5 for the 7,9-Dmhyp complex. A similar, yet different, situation obtains

(39) Lock, C. J. L.; Speranzini, R. A.; Powell, J. *Can. J. Chem.* **1976**, *54*, 53.
(40) Sinn, E.; Flynn, C. M.; Martin, R. B. *Inorg. Chem.* **1977**, *16*, 2403.
(41) Neidle, S.; Taylor, G. L.; Robins, A. B. *Acta Crystallogr., Sect. B* **1978**, *B34*, 1838.
(42) Melanson, R.; Rochon, F. D. *Inorg. Chem.* **1978**, *17*, 679.

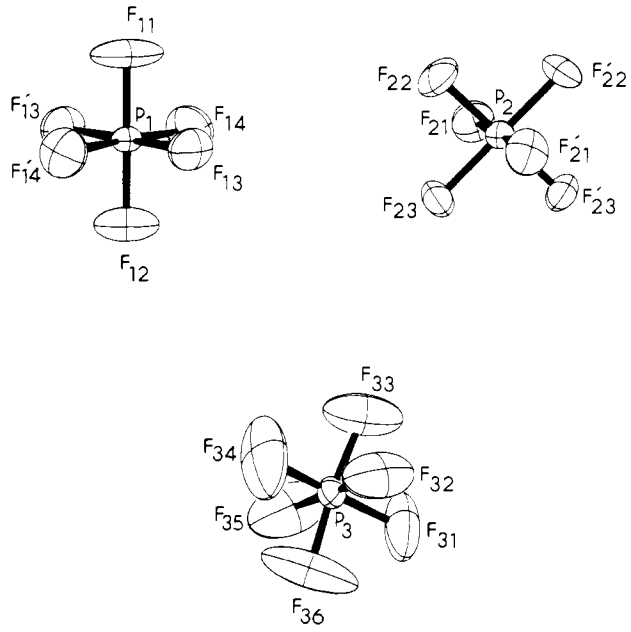

Figure 6. Perspective views of the three independent PF_6 anions in the hypoxanthine derivative. The PF_6 anions containing P(1) and P(2) possess twofold molecular symmetry.

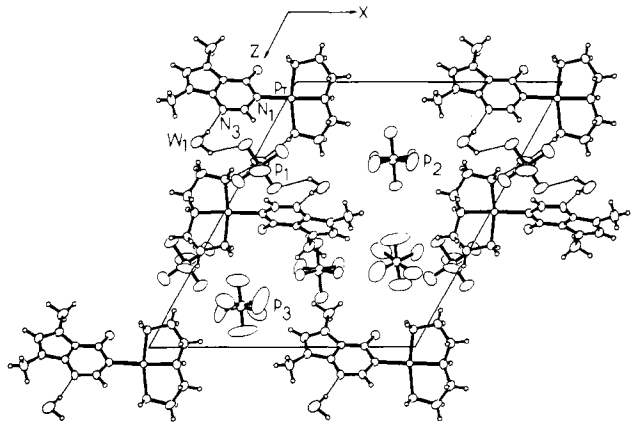

Figure 7. Projection view down *b* of the intermolecular interactions (thin lines) contained in the (010) plane in the [(dien)Pt(7,9-Dmhyp)]$(PF_6)_2$ structure.

for the N(7)-bound dien complexes of guanosine[34] and inosine;[35] there, the presence of the optically active sugar moiety yields diasteromers which crystallize in optically pure spacial arrays described by the space groups $P2_1$ (monoclinic, inosine complex)[34] and $P2_12_12_1$ (orthorhombic, guanosine complex).[35]

Cramer and Dahlstrom[43] have provided spectroscopic evidence (^1H and ^{13}C NMR data) for diastereomers of [(*N*,*N*,*N*′,*N*′-tetramethylethylenediamine)(guanosine)$_2$platinum(II)]$^{2+}$, where simple interconversion of isomers by a 180° rotation about the Pt(II)–N(7) bond is sterically inhibited by the bulky chelate ligand. In contrast, the interconversion of the two enantiomers of the N(1)-bound 7,9-Dmgua and 7,9-Dmhyp complexes does not involve rotation of the purine base through the coordination plane (a different stereoisomer of the complex results in that case for the dien complexes). The intramolecular interconversion of enantiomers in the N(1)-bound purine complexes surely involves a narcissistic reaction coordinate[44] [rotation about the Pt(II)–N(1) bond]. Ideally, the cations attain *m* (C_s) local symmetry in the transition state when the purine base is normal to the coordination plane.

Molecular Geometry of the 7,9-Dmgua and 7,9-Dmhyp Ligands. The bond lengths and angles in the N(1)-coordinated 7,9-Dmgua and 7,9-Dmhyp ligands are presented in Table V. Taking into account the minor differences expected from the presence of the exocylic amino group at position 2 of the 7,9-Dmgua ligand,[34,35,45] the geometries of the two ligands are in excellent agreement between themselves and also with those observed in a Cu(II) complex with 7,9-Dmhyp[1a] and in the salt of the 7,9-DmguaH$^+$ cation [N(1)-protonated 7,9-Dmgua] and the PF_6^- anion.[46]

The major difference in the molecular structures of the 7,9-dimethyl-6-oxopurines studies thus far lies in the endocyclic angles centered at N(1), C(6) and C(2) of the purine base. For the Pt(II) complexes with 7,9-Dmgua and 7,9-Dmhyp, the endocylic angle C(2)–N(1)–C(6) is 120.5 (5) and 121.5 (7)°, respectively. These values are in good agreement with that found in the Cu(II)–7,9-Dmhyp complex, (121.8 (3)°).[1a] In the 7,9-DmguaH$^+$ cation,[46] the value for this bond angle (126.3 (3)°) is significantly larger than found in the N(1)-coordinated Pt(II) and Cu(II) complexes just cited but similar to those found in guanosine and inosine[45] (124–125°), the protonated hypoxanthine base[47] (124.9 (1)°) and several N(7)-coordinated 9-methylhypoxanthine complexes[48,49] (124–126°). For methyl substitution at N(1) [as found, for example, in the modified purine base theophylline (1,3-dimethyl-2,6-dioxopurine)[50,51] and in the N(7)-coordinated theophylline monoanion[52–56]], the bond angle C(2)–N(1)–C(6) is ~126°. These observations are in agreement with the general conclusion[5,10,37,38] that metal coordination [specifically, Pt(II) and Cu(II) here] is less effective than a proton or an alkyl substituent in inducing molecular structural changes.

Consistent with the small C(2)–N(1)–C(6) endocyclic bond angle in the N(1)-bound coordination complexes is the enlarged N(1)–C(6)–C(5) bond angle [113.5 (5)° in the Pt(II)–7,9-Dmgua and 111.0 (6) and 110.0 (3)° for the Pt(II)– and Cu(II)–7,9-Dmhyp complexes] relative to that observed [109.3 (3)°] in the 7,9-DmguaH$^+$ cation.[46] Concomitantly, the endocyclic bond angle N(1)–C(2)–N(3) increases from 123.7 (3)° in the 7,9-DmguaH$^+$ cation[46] to near 128° in the three metal complexes concurrent with an increase of 0.02–0.03 Å in the N(1)–C(2) bond length.

As in most purine bases,[57] the nine-atom framework in the N(1)-bound 7,9-Dmgua and 7,9-Dmhyp ligands is significantly nonplanar (Tables VI and VII). The dihedral angle between a highly planar imidazole ring and a pyrimidine ring which retains some degree of nonplanarity is 3.5 (4)° for the 7,9-Dmgua base and 1.3 (4)° for the 7,9-Dmhyp base. The higher degree of nonplanarity in the 7,9-Dmgua complex might result from the increased interligand repulsion and Pt(II)···O(6) interaction in this complex cation, vide supra. In the two complex cations, the Pt(II) atoms and the exocylic carbonyl

(43) Cramer, R. E.; Dahlstrom, P. L. *J. Am. Chem. Soc.* **1979**, *101*, 3679.
(44) Salem, L.; Durup, J.; Bergeron, G.; Cazes, D.; Chapuisat, X.; Kagan, H. *J. Am. Chem. Soc.* **1970**, *92*, 4472.
(45) Thewalt, U.; Bugg, C. E.; Marsh, R. E. *Acta Crystallogr., Sect. B* **1970**, *B26*, 1089.
(46) de Castro, B.; Wilkowski, K.; Marzilli, L. G.; Kistenmacher, T. J., to be submitted for publication.
(47) Sletten, J.; Jensen, L. H. *Acta Crystallogr., Sect. B* **1969**, *B25*, 1608.
(48) Sletten, E. *Acta Crystallogr., Sect. B* **1974**, *B30*, 1961.
(49) Sletten, E.; Kaale, R. *Acta Crystallogr., Sect. B* **1977**, *B33*, 158.
(50) Sutor, D. J. *Acta Crystallogr.* **1958**, *11*, 83.
(51) Shefter, E. *J. Pharm. Sci.* **1971**, *58*, 710.
(52) Kistenmacher, T. J. *Acta Crystallogr., Sect. B* **1975**, *B31*, 85.
(53) Kistenmacher, T. J.; Szalda, D. J. *Acta Crystallogr., Sect. B* **1975**, *B31*, 90.
(54) Kistenmacher, T. J.; Szalda, D. J.; Marzilli, L. G. *Inorg. Chem.* **1975**, *14*, 1686.
(55) Szalda, D. J.; Kistenmacher, T. J.; Marzilli, L. G. *Inorg. Chem.* **1976**, *15*, 2783.
(56) Szalda, D. J.; Kistenmacher, T. J.; Marzilli L. G. *J. Am. Chem. Soc.* **1976**, *98*, 8371.
(57) Voet, D.; Rich, A. *Prog. Nucleic Acids Res. Mol. Biol.* **1970**, *10*, 103.

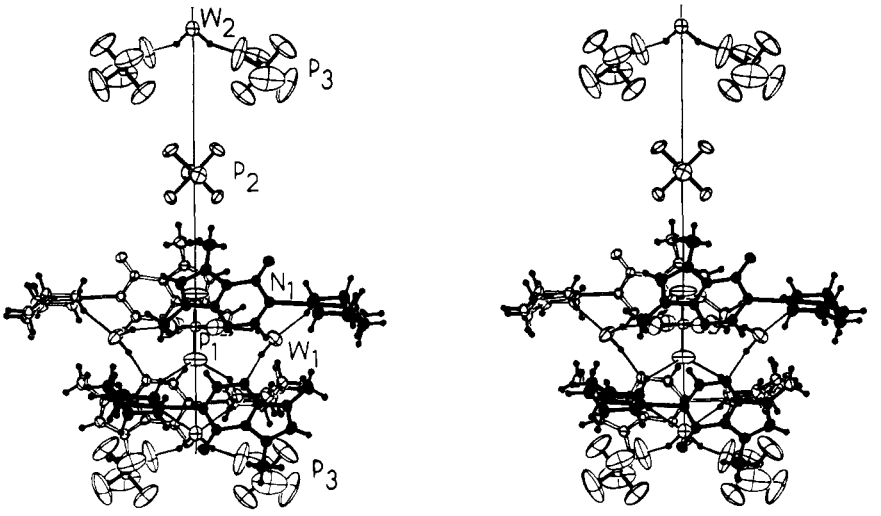

Figure 8. Stereoview of the interacting columns along *b* in the structure of [(dien)Pt(7,9-Dmhyp)]$(PF_6)_2$. Thin lines illustrate the intermolecular hydrogen bonding.

oxygen atom O(6) (Table VI and VII) show substantial deviations from the purine framework (0.33 and 0.08 Å for the 7,9-Dmgua complex and 0.26 and 0.07 Å for the 7,9-Dmhyp complex). In both instances, the deviations of the Pt(II) and O(6) atoms are to opposite sides of the plane of the base. In the Cu(II)–7,9-Dmhyp complex,[1a] the Cu(II) and O(6) atoms again show significant deviations from the plane of the purine base; in this case, however, with its more significant metal–O(6) intramolecular interaction, both atoms deviate to the same side of the purine ring.

Hexafluorophosphate Anions. In each of the structures reported here, there are two PF_6^- anions formally required per Pt(II) complex cation for charge neutrality. In the 7,9-Dmgua structure, the two independent PF_6^- anions (Figure 3) lie in general positions, and no symmetry elements of the idealized point group $m3m$ (O_h) for the PF_6^- anion are crystallographically required. In the 7,9-Dmhyp structure, one of the charge-balancing PF_6^- anions [containing the P atom labeled P(3)] (Figure 6) lies in a general position, and the other two independent PF_6^- anions lie on special positions with 2 (C_2) molecular symmetry required. Interestingly, one of these specially positioned PF_6^- anions [containing the P atom labeled P(1)] (Figure 6) utilizes one of its principal twofold axes [$C_2 = C_4^2$], while the second [containing the P atom labeled P(2)] (Figure 6) employs one of the secondary [C_2'] twofold axes of an idealized octahedron.[58]

The PF_6^- anions in both structres are relatively well behaved for an ion which is often found to be highly disordered.[59] For the general position PF_6^- anions of the 7,9-Dmgua structure, the P–F_{av} distances are 1.57 (3) and 1.59 (1) Å for the anions containing P(1) and P(2), respectively. The overall average P–F distance is 1.58 (2) Å, with individual values ranging from 1.53 to 1.61 Å. The average cis F–P–F angle for both anions in the 7,9-Dmgua structure is 90 (1)°, with individual values from 88 to 92°. The P–F bond lengths observed in these two anions (as well as those in the 7,9-Dmhyp structure) surely suffer some apparent shortening owing to the relatively large thermal motion indicated by their individual anisotropic thermal parameters. We have attempted to correct the P–F bond lengths utilizing the librational tensor obtained from a rigid-body analysis according to the method of Schomaker and Trueblood.[60] The RMS difference between the least-squares and the rigid-body thermal parameters was 0.02 Å^2, indicating that the PF_6^- groups can only in a limited sense be treated as rigid bodies.[60] Nonetheless, the "corrected" P–F_{av} distance shows a reasonable rise by 0.03–1.61 (2) Å. The corrections to the F–P–F bond angles are insignificant.

Similarly, we have treated the three independent PF_6^- anions in the 7,9-Dmhyp structure for thermal motion effects by the rigid-body method (RMS difference in the least-squares and rigid-body thermal parameters again of 0.02 Å). The uncorrected P–F_{av} bond length for these three PF_6^- anions was 1.54 (5) Å, with individual values ranging from 1.45 to 1.61 Å. The thermally "corrected" P–F_{av} distance is 1.60 (1) Å. The F–P–F angles are once again insensitive to the correction and average to 90 (5)°.

The corrected P–F_{av} distances derived here agree well with the P–F_{av} bond length [1.59 (1) Å] obtained from two studies on salts containing the PF_6^- anion at low temperature (87 K).[61,62] Our correction to the P–F_{av} bond distance employing the rigid-body method appear though to lead to a slight overestimate, as was found earlier by others,[63,64] [P–F_{av} = 1.63 (1) Å] using the riding model of Busing and Levy.[65]

Crystal Packing. A. [(dien)Pt(7,9-Dmgua)]$(PF_6)_2$. The crystal packing for [(dien)Pt(7,9-Dmgua)]$(PF_6)_2$ is presented in the stereoview of Figure 4. The structure is largely stabilized by electrostatic interactions between the complex cations and the hexafluorophosphate anions, although some hydrogen bonding interactions are also present (Table VIII) and expected to contribute to the crystal stabilization. Pairs of cationic complexes, related by inversion centers of the type ($^1/_2$, 0, $^1/_2$), form into dimeric units through the intercomplex hydrogen bonding between the exocylic carbonyl oxygen atom O(6) of the 7,9-Dmgua base and the proton off the central, secondary amino group of the dien chelate (Figure 4). Each of these dimers is then electrostatically coupled to six surrounding PF_6^- anions, which preferentially interact with the formally positive imidazole ring of the purine base. The

(58) Cotton, F. A. "Chemical Applications of Group Theory", 2nd ed.; Wiley-Interscience: New York, 1971.
(59) Brown, I. D.; Brown, M. C.; Hawthorne, F. C. "Bond Index to the Determination of Inorganic Crystal Structures"; McMaster University Press: Ontario, 1970–1979.
(60) Schomaker, V.; Trueblood, K. N. *Acta Crystallogr., Sect. B* **1968**, *B24*, 63.
(61) Olmstead, M. O.; Hope, H.; Benner, L. S.; Balch, A. L. *J. Am. Chem. Soc.* **1977**, *99*, 5502.
(62) Castro, J. M.; Hope, H. *Inorg. Chem.* **1978**, *17*, 1444.
(63) Goldberg, S. Z.; Eisenberg, R.; Miller, J. S. *Inorg. Chem.* **1977**, *16*, 1502.
(64) Cobbledick, R. E.; Einstein, F. W. B. *Acta Crystallogr., Sect. B* **1978**, *B34*, 1473.
(65) Busing, W. R.; Levy, H. A. *Acta Crystallogr.* **1964**, *17*, 142.

primary imidazole-PF_6^- interactions are through the methyl groups off N(9) and (7). There is also some evidence (Table VIII) that the terminal amino groups of the dien chelate form weak hydrogen bonds with two of the fluorine atoms of the P(1)-containing PF_6^- anion.

There seems to be no evidence of base-base stacking interactions in this largely ionic structure.

B. [(dien)Pt(7,9-Dmhyp)]$(PF_6)_2$·1.5H_2O. For this structure, three features dominate the crystal packing: Coulombic interactions between the ionic components, intermolecular hydrogen bonding, and a complex set of hydrogen bonds involving the waters of crystallization (Figures 7 and 8 and Table VIII). In describing this rather complex structure, we have divided the sets of interactions into two classes—those within the (010) crystallographic plane (Figure 7) and those which give rise to a columnar array along the [010] direction.

Within the (010) crystallographic plane, the complex cations are associated into dimeric pairs about the twofold axes along *b* (Figure 7). One of the specially positioned PF_6^- anions [P(1)] lies on the twofold axis along *b* and acts as a pivot for the coupling of two symmetry-related complex cations. Direct hydrogen bonding between the centrally located PF_6^- anion and one of the terminal amino groups of the dien chelate is observed, as well as a water bridge system utilizing the general position water molecule, W(1), and N(3) of the 7,9-Dmhyp base and the PF_6^- anion (Figure 7). Interactions between these dimeric units are mainly electrostatic in nature, with the methyl substituents off the imidazole ring of the purine ligand primarily involved.

Joining these highly interactive planes are columnar arrays (Figure 8) paralleling the crystallographic *b* axis. The sequence of components along this columnar array is as follows: (a) the specially positioned PF_6^- anion containing P(1) associated with two complex cations and water, W(1), molecules through hydrogen bonds, (b) the specially positioned PF_6^- anion containing P(2) which is electrostatically coupled to the methyl substituents of the purine bases associated with the P(1) PF_6^- anion, and finally, (c) the water molecule W(2) which is positioned on the twofold axis and hydrogen bonded to two general position PF_6^- anions, P(3).

Again, as in the 7,9-Dmgua structure, there is no evidence of base-base stacking interactions in the 7,9-Dmhyp crystal structure.

Summary

We find that the complex cations [(dien)Pt(7,9-Dmgua)]$^{2+}$ and [(dien)Pt(7,9-Dmhyp)]$^{2+}$ provide the first examples of type I Pt(II)-N(1)-bound 6-oxopurine complexes. Intramolecular interligand hydrogen bonding and Pt···O(6) interactions are integral features of both complexes. Intracomplex hydrogen bonding is the more important of the two interactions in the 7,9-Dmhyp complex, while the Pt···O(6) distance is shorter in the 7,9-Dmgua complex. The Pt···O(6) interaction in the 7,9-Dmgua complex is similar in apparent strength to that found in several Pt(II)-cytosine systems but substantially stronger than observed in type I Pt(II)-N(7)-bound 6-oxopurine complexes. The difference in the mode of interaction of the (dien)Pt moiety and the 7,9-Dmgua and 7,9-Dmhyp bases is proposed to arise largely as a consequence of the changes in molecular geometry needed to relieve the steric strain between the 2-amino substituent of the 7,9-Dmgua ring and the (dien)Pt group. In addition to its role in the interligand hydrogen bonding and the Pt(II) binding, O(6) of each base participates in intercomplex hydrogen bonding in the crystalline state. Otherwise, the crystal structures encompass general coulombic forces as well as complex hydrogen bonding arrays to achieve stability.

Acknowledgment. This investigation was supported by the National Institutes of Health, Public Health Service Grants GM 20544 and GM 29222. We thank Matthey Bishop, Inc., for a loan of K_2PtCl_4.

Registry No. [(dien)(7,9-Dmgua)Pt^{II}]$(PF_6)_2$, 76900-59-9; [(dien)(7,9-Dmhyp)Pt^{II}]$(PF_6)_2$·1.5H_2O, 76915-23-6; Pt(dien)I_2, 18509-61-0.

Supplementary Material Available: Tables of nonhydrogen atom anisotropic thermal parameters and parameters for the hydrogen atoms and a list of calculated and observed structure factor amplitudes (77 pages). Ordering information is given on any current masthead.

Contribution from the Department of Chemistry, Massachusetts Institute of Technology, Cambridge, Massachusetts 02139

Preparation and Reactions of $[ZrCl_3(PR_3)_2]_2$ (R = Et, Pr, Bu) and X-ray Structure of $[ZrCl_3(PBu_3)_2]_2$

JEFFREY H. WENGROVIUS, RICHARD R. SCHROCK,*[1] and CYNTHIA S. DAY

Received October 30, 1980

Complexes of the type $[ZrCl_3(PR_3)_2]_2$ (R = Et, Pr, Bu) have been prepared in high yield by reducing $ZrCl_4(PR_3)_2$ with 1 equiv of sodium amalgam. The X-ray structure of $[ZrCl_3(PBu_3)_2]_2$ shows it to be a chloride-bridged dimer with a Zr-Zr bond distance of 3.182 (1) Å. $[ZrCl_3(PBu_3)_2]_2$ crystallizes in the monoclinic space group $C2/c$ with a = 26.570 (6) Å, b = 15.287 (3) Å, c = 16.452 (3) Å, and β = 97.18 (2)°. The structure was solved by standard Patterson and difference-Fourier methods to values of R_1 = 5.3% and R_2 = 6.2% for 4720 reflections having $2\theta_{Mo K\alpha} < 55°$ and $I > 3\sigma(I)$. The molecule has a distorted octahedral geometry about each Zr and cis phosphine ligands in the same plane as the bridging chloride ligands. $[ZrCl_3(PR_3)_2]_2$ reacts with ethylene and propylene to give Zr(IV) complexes, $(PR_3)_2Cl_3ZrCH_2CHRZrCl_3(PR_3)_2$ (R = H or Me). On reaction with butadiene, $[ZrCl_3(PEt_3)_2]_2$ disproportionates to $ZrCl_4(PEt_3)_2$ and $ZrCl_2(\eta^6\text{-}C_8H_{12})(PEt_3)$; $\eta^6\text{-}C_8H_{12}$ is the well-known bis allyl ligand formed by coupling two butadiene molecules.

Introduction

We recently reported[2] our unsuccessful attempts to prepared a zirconium-neopentylidene complex by promoting loss of neopentane from $Zr(CH_2CMe_3)_2Cl_2(PMe_3)_2$ thermally or photochemically. Photolysis gave a sparingly soluble, forest green crystalline product with the composition $ZrCl_3(PMe_3)_2$ in ca. 60% yield vs. Zr. Since this compound was diamagnetic and showed only PMe_3 ligands by ^1H NMR, we proposed it was dimeric with a Zr-Zr bond and two bridging chloride ligands. This would be the first example of a complex containing a Zr-Zr bond and the only member so far of the class of adducts of β-$ZrCl_3$ which is nicely soluble and easy to

(1) To whom correspondence should be addressed.
(2) Wengrovius, J. H.; Schrock, R. R. *J. Organomet. Chem.* **1981**, *205*, 319-322.

0020-1669/81/1320-1844$01.25/0